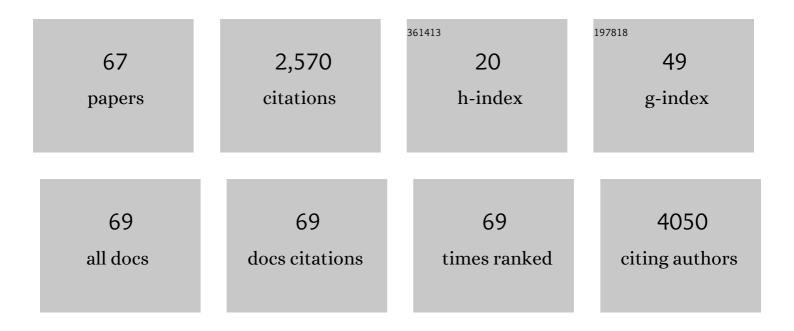
List of Publications by Year in descending order

Source: https://exaly.com/author-pdf/13649/publications.pdf Version: 2024-02-01



PILLO R VAN HEESWILK

#	Article	IF	CITATIONS
1	The Cardiomyocyte in Heart Failure with Preserved Ejection Fraction—Victim of Its Environment?. Cells, 2022, 11, 867.	4.1	1
2	The Road Toward Reproducibility of Parametric Mapping of the Heart: A Technical Review. Frontiers in Cardiovascular Medicine, 2022, 9, .	2.4	10
3	Compressed sensing with signal averaging for improved sensitivity and motion artifact reduction in fluorineâ€19 MRI. NMR in Biomedicine, 2021, 34, e4418.	2.8	8
4	Multi-energy photon-counting computed tomography versus other clinical imaging techniques for the identification of articular calcium crystal deposition. Rheumatology, 2021, 60, 2483-2485.	1.9	20
5	A robust broadband fatâ€suppressing phaser T 2 â€preparation module for cardiac magnetic resonance imaging at 3T. Magnetic Resonance in Medicine, 2021, 86, 1434-1444.	3.0	2
6	Cardiac magnetic resonance imaging with T2 mapping for the monitoring of acute heart transplant rejection in patients with problematic endomyocardial biopsy: in anticipation of new recommendations. Kardiologia Polska, 2021, 79, 339-343.	0.6	4
7	Oxygen-sensitive Magnetic Resonance Imaging: A Noninvasive Step Forward for Diagnosing Vasculopathy in the Cardiac Allograft. Transplantation, 2021, 105, 1664-1665.	1.0	1
8	Respiratory Motion-Registered Isotropic Whole-Heart T2 Mapping in Patients With Acute Non-ischemic Myocardial Injury. Frontiers in Cardiovascular Medicine, 2021, 8, 712383.	2.4	3
9	Endogenous assessment of myocardial injury with single-shot model-based non-rigid motion-corrected T1 rho mapping. Journal of Cardiovascular Magnetic Resonance, 2021, 23, 119.	3.3	14
10	Standards for writing Society for Cardiovascular Magnetic Resonance (SCMR) endorsed guidelines, expert consensus, and recommendations: a report of the publications committee. Journal of Cardiovascular Magnetic Resonance, 2021, 23, 129.	3.3	2
11	A characterization of ABLâ€101 as a potential tracer for clinical fluorineâ€19 MRI. NMR in Biomedicine, 2020, 33, e4212.	2.8	9
12	Quantification of myocardial interstitial fibrosis and extracellular volume for the detection of cardiac allograft vasculopathy. International Journal of Cardiovascular Imaging, 2020, 36, 533-542.	1.5	10
13	Scalable Learning-Based Sampling Optimization for Compressive Dynamic MRI. , 2020, , .		11
14	T2 Mapping from Super-Resolution-Reconstructed Clinical Fast Spin Echo Magnetic Resonance Acquisitions. Lecture Notes in Computer Science, 2020, , 114-124.	1.3	2
15	Accelerated and highâ€resolution cardiac <scp>T</scp> ₂ mapping through peripheral kâ€space sharing. Magnetic Resonance in Medicine, 2019, 81, 220-233.	3.0	6
16	Noncontrast free-breathing respiratory self-navigated coronary artery cardiovascular magnetic resonance angiography at 3 T using lipid insensitive binomial off-resonant excitation (LIBRE). Journal of Cardiovascular Magnetic Resonance, 2019, 21, 38.	3.3	15
17	A blackâ€blood ultraâ€short echo time (UTE) sequence for 3D isotropic resolution imaging of the lungs. Magnetic Resonance in Medicine, 2019, 81, 3808-3818.	3.0	6
18	In vitro optimization and comparison of CT angiography versus radial cardiovascular magnetic resonance for the quantification of cross-sectional areas and coronary endothelial function. Journal of Cardiovascular Magnetic Resonance, 2019, 21, 11.	3.3	3

#	Article	IF	CITATIONS
19	Towards Quantification of Inflammation in Atherosclerotic Plaque in the Clinic – Characterization and Optimization of Fluorine-19 MRI in Mice at 3 T. Scientific Reports, 2019, 9, 17488.	3.3	10
20	Simultaneous fatâ€free isotropic 3D anatomical imaging and T ₂ mapping of knee cartilage with lipidâ€insensitive binomial offâ€resonant RF excitation (LIBRE) pulses. Journal of Magnetic Resonance Imaging, 2019, 49, 1275-1284.	3.4	11
21	Improved respiratory selfâ€navigation for 3D radial acquisitions through the use of a pencilâ€beam 2Dâ€T ₂ â€prep for freeâ€breathing, wholeâ€heart coronary MRA. Magnetic Resonance in Medicine, 2018, 79, 1293-1303.	3.0	3
22	Isotropic threeâ€dimensional <i>T</i> ₂ mapping of knee cartilage: Development and validation. Journal of Magnetic Resonance Imaging, 2018, 47, 362-371.	3.4	21
23	Chemical shift encoding (CSE) for sensitive fluorineâ€19 MRI of perfluorocarbons with complex spectra. Magnetic Resonance in Medicine, 2018, 79, 2724-2730.	3.0	19
24	A chemical shift encoding (CSE) approach for spectral selection in fluorineâ€19 MRI. Magnetic Resonance in Medicine, 2018, 79, 2183-2189.	3.0	10
25	On the accuracy and precision of cardiac magnetic resonance T ₂ mapping: A highâ€resolution radial study using adiabatic T ₂ preparation at 3 T. Magnetic Resonance in Medicine, 2017, 77, 159-169.	3.0	16
26	Fluorinated Mesoporous Silica Nanoparticles for Binuclear Probes in ¹ H and ¹⁹ F Magnetic Resonance Imaging. Langmuir, 2017, 33, 10531-10542.	3.5	21
27	T2 Relaxation Time Varies Within the Load-Bearing Regions of Non-OA Femoral Cartilage. Osteoarthritis and Cartilage, 2017, 25, S249-S250.	1.3	0
28	Three-Dimensional Self-Navigated T2 Mapping for the Detection of Acute Cellular Rejection After Orthotopic Heart Transplantation. Transplantation Direct, 2017, 3, e149.	1.6	12
29	Characterization of perfluorocarbon relaxation times and their influence on the optimization of fluorine-19 MRI at 3 tesla. Magnetic Resonance in Medicine, 2017, 77, 2263-2271.	3.0	25
30	Clinical recommendations for cardiovascular magnetic resonance mapping of T1, T2, T2* and extracellular volume: A consensus statement by the Society for Cardiovascular Magnetic Resonance (SCMR) endorsed by the European Association for Cardiovascular Imaging (EACVI). Journal of Cardiovascular Magnetic Resonance, 2017, 19, 75.	3.3	1,074
31	Apparent Diffusion coefficient (ADC), T1 and T2 quantitative indexes of the myocardium in athletes before, during and after extreme mountain ultra-marathon: correlation with myocardial damages and inflammation biomarkers. Journal of Cardiovascular Magnetic Resonance, 2016, 18, O41.	3.3	0
32	Hyperpolarized ⁶ Li as a probe for hemoglobin oxygenation level. Contrast Media and Molecular Imaging, 2016, 11, 41-46.	0.8	15
33	Breath-held high-resolution cardiac T2 mapping with SKRATCH. Journal of Cardiovascular Magnetic Resonance, 2016, 18, P27.	3.3	0
34	Initial experience with isotropic 3D cardiac T2 mapping for the monitoring of cardiac allograft rejection. Journal of Cardiovascular Magnetic Resonance, 2016, 18, W23.	3.3	0
35	lsotropic three-dimensional T2 mapping of knee cartilage with T2-prepared segmented gradient ECHO at 3T. Osteoarthritis and Cartilage, 2016, 24, S300-S301.	1.3	0

36 Chapter 7 Cardiac Disease. , 2016, , 191-220.

#	Article	IF	CITATIONS
37	Repositioning precision of coronary arteries measured on X-ray angiography and its implications for coronary MR angiography. Journal of Magnetic Resonance Imaging, 2015, 41, 1251-1258.	3.4	3
38	Freeâ€running 4D wholeâ€heart selfâ€navigated golden angle MRI: Initial results. Magnetic Resonance in Medicine, 2015, 74, 1306-1316.	3.0	91
39	Combined T ₂ â€preparation and twoâ€dimensional pencilâ€beam inner volume selection. Magnetic Resonance in Medicine, 2015, 74, 529-536.	3.0	10
40	Selfâ€navigated isotropic threeâ€dimensional cardiac T ₂ mapping. Magnetic Resonance in Medicine, 2015, 73, 1549-1554.	3.0	51
41	Fluorine MR Imaging of Inflammation in Atherosclerotic Plaque in Vivo. Radiology, 2015, 275, 421-429.	7.3	50
42	Ultra-high-resolution 3D imaging of atherosclerosis in mice with synchrotron differential phase contrast: a proof of concept study. Scientific Reports, 2015, 5, 11980.	3.3	14
43	Accelerated and KWIC-filtered cardiac T2 mapping for improved precision: proof of principle. Journal of Cardiovascular Magnetic Resonance, 2015, 17, .	3.3	2
44	Respiratory Self-navigated Postcontrast Whole-Heart Coronary MR Angiography: Initial Experience in Patients. Radiology, 2014, 270, 378-386.	7.3	96
45	Fat signal suppression for coronary MRA at 3T using a water-selective adiabatic T2-preparation technique. Magnetic Resonance in Medicine, 2014, 72, spcone-spcone.	3.0	0
46	Free-breathing T2 mapping at 3T for the monitoring of cardiac allograft rejection: initial results. Journal of Cardiovascular Magnetic Resonance, 2014, 16, M11.	3.3	1
47	Numerically optimized radiofrequency pulses for robust and low-power cardiovascular T2 preparation at 3T. Journal of Cardiovascular Magnetic Resonance, 2014, 16, P41.	3.3	Ο
48	Radial cardiac T2 mapping with alternating T2 preparation intrinsically introduces motion correction. Journal of Cardiovascular Magnetic Resonance, 2014, 16, P28.	3.3	0
49	Fat signal suppression for coronary MRA at 3T using a waterâ€selective adiabatic T ₂ â€preparation technique. Magnetic Resonance in Medicine, 2014, 72, 763-769.	3.0	13
50	Self-Navigation with Compressed Sensing for 2D Translational Motion Correction in Free-Breathing Coronary MRI: A Feasibility Study. PLoS ONE, 2014, 9, e105523.	2.5	17
51	Improved fat signal suppression for coronary MRA at 3T using a water-selective adiabatic T2-Prep technique. Journal of Cardiovascular Magnetic Resonance, 2013, 15, O5.	3.3	Ο
52	Self-navigated three-dimensional cardiac T2 mapping at 3T. Journal of Cardiovascular Magnetic Resonance, 2013, 15, P51.	3.3	0
53	Selective In Vivo Visualization of Immune-Cell Infiltration in a Mouse Model of Autoimmune Myocarditis by Fluorine-19 Cardiac Magnetic Resonance. Circulation: Cardiovascular Imaging, 2013, 6, 277-284.	2.6	60
54	Free-Breathing 3 T Magnetic Resonance T2-Mapping of the Heart. JACC: Cardiovascular Imaging, 2012, 5, 1231-1239.	5.3	75

#	Article	IF	CITATIONS
55	Motion Compensation Strategies in Magnetic Resonance Imaging. Critical Reviews in Biomedical Engineering, 2012, 40, 99-119.	0.9	49
56	Quantitative free-breathing 3T T2-mapping of the heart designed for longitudinal studies. Journal of Cardiovascular Magnetic Resonance, 2012, 14, .	3.3	0
57	A comparison of in vivo ¹³ C MR brain glycogen quantification at 9.4 and 14.1 T. Magnetic Resonance in Medicine, 2012, 67, 1523-1527.	3.0	9
58	Fluorine-19 Magnetic Resonance Angiography of the Mouse. PLoS ONE, 2012, 7, e42236.	2.5	25
59	Quantification of brain glycogen concentration and turnover through localized ¹³ C NMR of both the C1 and C6 resonances. NMR in Biomedicine, 2010, 23, 270-276.	2.8	19
60	Feasibility of in vivo15N MRS detection of hyperpolarized 15N labeled choline in rats. Physical Chemistry Chemical Physics, 2010, 12, 5818.	2.8	96
61	Hyperpolarized lithiumâ€6 as a sensor of nanomolar contrast agents. Magnetic Resonance in Medicine, 2009, 61, 1489-1493.	3.0	53
62	Producing over 100ml of highly concentrated hyperpolarized solution by means of dissolution DNP. Journal of Magnetic Resonance, 2008, 194, 152-155.	2.1	39
63	Nonâ€invasive quantification of brain glycogen absolute concentration. Journal of Neurochemistry, 2008, 107, 1414-1423.	3.9	24
64	Serial in vivo MR tracking of magnetically labeled neural spheres transplanted in chronic EAE mice. Magnetic Resonance in Medicine, 2007, 57, 164-171.	3.0	89
65	Relaxivity of Gd-based contrast agents on X nuclei with long intrinsic relaxation times in aqueous solutions. Magnetic Resonance Imaging, 2007, 25, 821-825.	1.8	15
66	MR Evaluation of the Glomerular Homing of Magnetically Labeled Mesenchymal Stem Cells in a Rat Model of Nephropathy. Radiology, 2006, 238, 200-210.	7.3	133
67	Relaxivity of liposomal paramagnetic MRI contrast agents. Magnetic Resonance Materials in Physics, Biology, and Medicine, 2005, 18, 186-192.	2.0	128